

MICROPHYSICS OF EUROPA'S SURFACE USING GALILEO/NIMS DATA. G. Cruz Mermy¹, F. Schmidt^{1,2}, F. Andrieu¹, I. Belgacem⁴, T. Cornet³ and N. Altobelli⁴, ¹ GEOPS, CNRS, Université Paris-Saclay, Rue du Belvédère, Bât. 504, 91405 Orsay, France. ² Institut Universitaire de France. ³ Aurora Technology BV for ESA. ⁴ European Space Agency (ESA), European Space Astronomy Centre (ESAC), Camino Bajo del Castillo s/n, 28692 Villanueva de la Cañada, Madrid, Spain.

Contact : guillaume.cruz-mermy@universite-paris-saclay.fr

Introduction: Europa's surface is one of the youngest surfaces in the solar system. The great diversity of morphologies observed quickly raised the question of the processes responsible for this active resurfacing. The Jovian moon is believed to hide a global liquid water ocean under its ice crust [1] which led to the assumptions of exchange between the surface and the putative subsurface ocean through cryovolcanism or diapirism events [1]. In addition, Europa is exposed to intense space weathering due to the continuous bombardment by electrons and ions from Jupiter's magnetosphere [2]. This strongly affects the surface composition as evidenced by the trailing hemisphere which appears darker and redder than the leading hemisphere. The surface therefore appears as the key witness of these internal and external processes, its characterization is essential to our understanding of Europa over geological time but also of its current habitability.

In the recent years our knowledge of Europa's surface composition has increased significantly, mainly through reflectance spectroscopy. Apart from water ice, present in both amorphous and crystalline form, linear mixture modelling allowed the detection of hydrated compounds such as hydrated sulfuric acid [2] and hydrated salts [3]. These detections reinforced the debate between a contribution by external sources or an endogenic production.

Spectral fitting analysis are great tools to demonstrate the presence of a compound. However, to determine precise abundance, one has to finely characterized the microphysics of the ice, such as average grain size, macroscopic roughness, porosity and endmember abundances which are highly degenerated with each other [4]. It is necessary to use radiative transfer modelling to estimate these parameters and integrating the highly nonlinear effects of the light path within the regolith due to scattering. Such models (for instance [5] and [6]) are based on the optical properties of the considered species and physical properties of the regolith. Here we report the use of the Douté model [6] in a Bayesian inference framework to retrieve microphysical properties of Europa's surface based on the Galileo Near-Infrared Mapping Spectrometer (NIMS; [7]) hyperspectral data.

Data: We use data acquired by NIMS collected during the Galileo Mission. As the mission was designed to perform flybys, the spatial resolution varies greatly from one cube to another which greatly limits the use of

several cubes for the same geographical area. We focus on high spatial resolution cubes (below 5 km/px) on both the leading and trailing hemisphere. Here, we present the analysis of calibrated data from the hyperspectral cube "14e006ci" (available from the PDS archive). We selected a spectrum that corresponds to a brighter surface close to a dark lineament of the trailing Anti-Jovian hemisphere (Fig. 1).

The estimated signal-to-noise ratio (SNR) is between 5 and 50. We mainly focus on the 0.9-2.5 μm region for which the SNR is higher but also because the optical constants of some compounds (hydrated salts and SAO) are not available beyond 2.5 μm . On this spectral range the uncertainty on the absolute calibration is up to 10% [7].

Radiative transfer model we use requires the optical constants of the species considered. Here we mainly use crystalline and amorphous water ice [8,9], sulfuric acid octahydrate (SAO; [2]), hydrated salts such as hexahydrite, bloedite and epsomite [10] and a dark compounds such as magnetite [11].

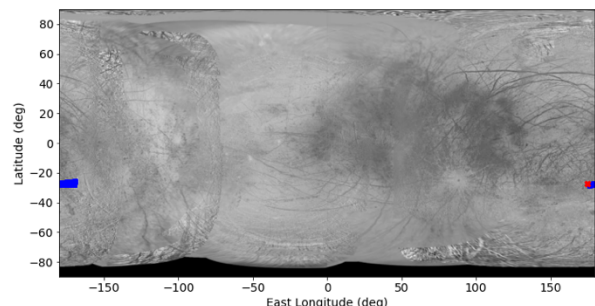


Figure 1 – Map of Europa with the studied area in blue (observation 14e006ci). The location of the spectrum used here is shown in red.

Method: We use a Monte Carlo Bayesian inference approach to analyze NIMS spectra because it has the advantage of allowing the exploration of a large parameter space and looking for non-unique solutions while statistically constraining the model parameters [12,13].

We use the Douté model [6], which allows estimate the bidirectional reflectance of the regolith according to the observation geometry of the data, the single scattering albedo, the particle phase function and the porosity coefficient. Then, the Bayesian Posterior sampling is used to sample the parameter space we wish to explore

by generating a large amounts of forward model spectra and select samples for which the model fit best the data. The parameters we are fitting for are the abundances, the grain size of each species and the macroscopic roughness of the regolith. For the abundances we use a Dirichlet prior to ensure that they are sum up to 1, while we use a uniform distribution for the other parameters.

The different steps follows : (1) a random set of parameters are sampled using the prior distribution function; (2) from these parameters, a forward simulation generate a spectrum at high spectral resolution spectrum from the forward model; (3) the spectrum is convolved with the instrument response function [7]; (4) the modelled spectrum is compared to the data using a likelihood probability function to compute the posterior probability of this set of parameters; (5) based on the comparison with the actually observed spectrum, this sample is kept following the posterior probability, or not. Once the chain of solutions is statistically stationary, its density represents the *a posteriori* probability density function of the parameters we seek to constrain. One can then get marginalized posterior distribution of the parameters as well as pairwise distribution to look at potential correlations between parameters.

Results: A typical result is shown figure 2 for one spectrum using 4 compounds : crystalline water ice, hexahydrite, magnetite and SAO. Looking at the residuals, one can see that the model provides an excellent fit to the data. The posterior distributions of abundances are also shown for the abundances and grain size (Fig. 3). In this case, hexahydrite seems to be the main compounds with its abundance constrained as $0.82 \pm 0.03/-0.04$ (median value with lower and upper equivalent 1σ) and a grain size of $3700 \pm 500/-400 \mu\text{m}$. Crystalline water ice is the second compound with its abundances constrained as 0.10 ± 0.02 and a grain size of $500 \pm 100/-70 \mu\text{m}$. SAO and magnetite are both very scarce with a median abundance of 0.04 ± 0.02 . The grain size of SAO well constrained with a value of $90 \pm 6 \mu\text{m}$ in contrast to magnetite grain size with a value of $630 \pm 930/-450 \mu\text{m}$ as showed figure 3.

Conclusion: In the light of these preliminary results, hexahydrite seems to be the major compound, with about 80% of volumetric abundance. The presence of hydrated salt close to dark lineaments at the trailing Anti-Jovian hemisphere location is consistent with [14]. Given the relatively small size of the grains (around 1cm), this enrichment may be due to external processes (sputtering) and may not be representative of the full ice shell of Europa.

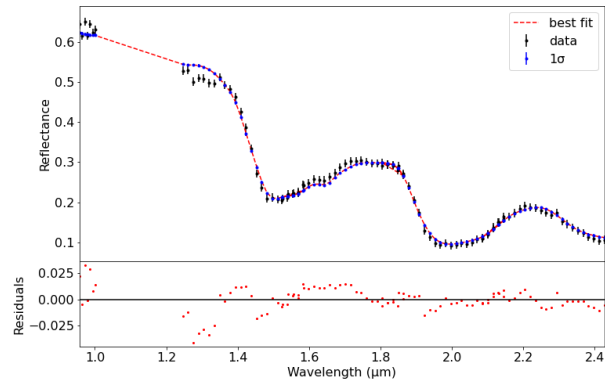


Figure 2- Results from analysis of a spectrum from observation "14e006ci" (-27.65°N, 175.00°E). This top plot shows the best fit (in red) for the fit to data (dark, with 1 sigma noise). The bottom plot shows the residuals.

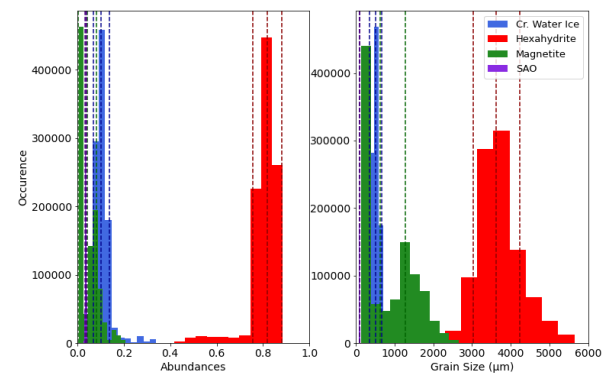


Figure 3 -. Plots of the posterior distributions for the abundances (left) and grain size (right). The dashed lines are the median values and 1 sigma upper and lower bounds.

References:

- [1] Pappalardo, R. et al. (1999) JGR, 104, 24015–24055.
- [2] Carlson, R. W. et al. (2005) Icar, 177, 461.
- [3] McCord, T. B. et al. (1998) Sci, 280, 1242.
- [4] Mishra, I. et al. (2021) Planet. Sci., 2, 183.
- [5] Hapke, B. (2012). Cambridge : Cambridge Univ. Press, 221.
- [6] Douté, S. and Schmitt, B. (1998) JGR, 103, 31367–31389.
- [7] Carlson, R. et al. (1992) ed. C. T. Russell, 457.
- [8] Schmitt, B. et al. (2004) SSHADE/GhoSST (OSUG Data Center).
- [9] Mastrapa, R. M. et al. (2009) ApJ, 701, 1447.
- [10] Dalton, J.B. et al. (2012) JGRE, 117, E03003.
- [11] Roush, T. et al. (2021) Icar, 361.
- [12] Mosegaard, K. et al. (1995) JGR, 100.B7, 12431–12447.
- [13] Schmidt, F. and Bourguignon, S. (2019) Icar, 317, 10–26.
- [14] McCord, T. B. et al. (2010) Icar, 209, 639–650.